PAPER • OPEN ACCESS

The penumbral solar filaments from the photosphere to the chromosphere

View the article online for updates and enhancements.

The penumbral solar filaments from the photosphere to the chromosphere

M Murabito[1], I Ermolli[1], F Giorgi[1], M Stangalini[1], S L Guglielmino[2], S Jafarzadeh[3,4], H Socas-Navarro[5,6] P Romano[7], F Zuccarello [2]

[1] INAF-Osservatorio astronomico di Roma, Via frascati, 33, 00078, Monteporzio Catone, Italy
[2] Dipartimento di Fisica e Astronomia "Ettore Majorana" - Sezione Astrofisica, Università degli Studi di Catania, Via S. Sofia 78, I-95123 Catania, Italy
[3] Rosseland Centre for Solar Physics, University of Oslo, P.O. Box 1029 Blindern, NO-0315 Oslo, Norway
[4] Institute of Theoretical Astrophysics, University of Oslo, P.O. Box 1029 Blindern, NO-0315 Oslo, Norway
[5] Instituto de Astrofísica de Canarias, 38205, C/ Via Láctea s/n, La Laguna, Tenerife, Spain
[6] Departamento de Astrofísica, Universidad de La Laguna, 38205, C/ Via Láctea s/n, La Laguna, Tenerife, Spain
[7] INAF-Osservatorio Astrofisico di Catania, Via S. Sofia, 78, 95123, Catania, Italy

E-mail: `mariarita.murabito@inaf.it`

Abstract. The magnetic field structure of sunspots above the photosphere remain poorly understood due to limitations in observations and the complexity of these atmospheric layers. In this regard, we studied the large isolated sunspot ($70'' \times 80''$) located in the active region NOAA 12546 with spectro-polarimetric measurements acquired along the Fe I 617.3 nm and Ca II 854.2 nm lines with the IBIS/DST instrument, under excellent seeing conditions lasting more than three hours. Using the Non Local Thermodynamic Equilibrium inversion code we inverted both line measurements simultaneously to retrieve the three-dimensional magnetic and thermal structure of the penumbral region from the bottom of the photosphere to the middle chromosphere. The analysis of data acquired at spectral ranges unexplored allow us to show clear evidence of the spine and intra-spine structure of the magnetic field at chromospheric heights. In particular, we found a peak-to-peak variations of the magnetic field strength and inclination of about 200 G and 10° chromospheric heights, respectively, and of about 300 G and 20° in the photosphere. We also investigated the structure of the magnetic field gradient in the penumbra along the vertical and azimuthal directions, confirming previous results reported in the literature from data taken at the spectral region of the He I 1083 nm triplet.

1. Introduction

Sunspots are the most important manifestation of the solar magnetism. They appear on the photosphere as dark structures composed by a dark region, called *umbra*, cooler than the unmagnetized Sun, and a radial and filamentary surrounding area called *penumbra*. High-resolution observations of penumbra formation are not easy to acquire and the physical processes involved remain poorly understood [2,3]. In particular, the flow patterns around the pore before and after the formation of the penumbra are still widely dibated. The results reported in [4,5] indicate the presence of a flow pattern of opposite sign with respect to the typical Evershed flow pattern before the penumbra formation occurs. The usual place where the penumbra

formation starts to form also represents a reason for debate. In fact, in [6] the first high-resolution observations catching the overall phase of the penumbra formation, arguing that the flux emergence undergoing between the opposite polarities area in an Active Region (AR) prevents the formation of a stable penumbra. In contrast, [5, 7] showed that it is possible to observe the formation of stable penumbra even in the area between the two main polarities of sunspot region.

Prolonged datasets on the filamentary structure of the penumbra became available only recently [8], by using space-borne observations acquired by the *Hinode* satellite, therefore solving most of the long-lasting controversies. In particular, these recent observations highlighted that the filaments consist of bright heads, the part of the filaments nearest to the sunspot umbra, with same polarity of the umbra, enhanced ($\approx 1.5 - 2$ kG) and more vertical ($\approx 35°$) magnetic filed than the field observed along the filament axis (≈ 1 kG and $70°$), respectively. Moreover, the filament tails, the farthest part of the filaments from the sunspot umbra, are characterized by stronger fields ($\approx 2 - 3.5$ kG) than umbra [8], and with opposite polarity. The above described filament configuration is called *spine* (more vertical and stronger fields) and *intra-spine* (more horizontal and weaker fields) structure and it is typically observed at photospheric heights.

However, most of the information concerning the magnetic field of the penumbral filaments derive from photospheric observations. Until the work by [9], the only chromospheric diagnostic employed to investigate penumbrae at higher atmospheric heights was the He I triplet at 1083 nm. Analyzing penumbral observations in this spectral region, [10] reported the presence of the small-scale spine-intraspine structure in the magnetic field inclination alone.

In this contribution, we report the analysis of the chromospheric penumbral magnetic field configuration derived from a multi-line NICOLE inversion of photospheric and chromospheric spectral lines.

2. Observations and Data analysis

AR NOAA 12546 was observed with the Interferometric Bidimensional Spectrometer (IBIS, [11]), installed at the Dunn Solar Telescope (DST, Sacramento Peak, New Mexico), on 2016 May 20 for about 3 hours under excellent seeing conditions. The observations were carried out on the positive and mature sunspot within this AR, located near the disk center. This sunspot is the largest sunspot appeared during the solar cycle 24. The data set consists of spectro-polarimetric measurements along the Fe I 617.3 nm and Ca II 854.2 nm lines with a cadence of 48 s. Data were taken at 21 spectral points, with a spectral sampling 20 mÅ and 60 mÅfor the iron and calcium line profiles, respectively. The full field of view (FOV) is 500×1000 pixels with a pixel scale of $0.08''$. For further details about these observations and data reduction, see [12] and [1]. In this contribution we report results obtained from the best seeing scan of the time series.

To derive the parameters of the magnetic field, we used the Non-LTE inversion COde using the Lorien Engine (NICOLE, [13]. The inversion was run by using as a reference the inversion reported in [14]. In particular, we used five equidistant nodes for the temperature, three nodes for each component of the vector magnetic field, two nodes for the line-of-sigth (LOS) velocity and one node for both the micro- and macro-turbulence. As initial model, we assumed the FALC atmosphere [16] where we modified the values of the longitudinal component of the magnetic field (B_z) with a constant value of 1.5 kG. The NICOLE code applies a NLTE treatment of the Radiative Transfer Eqaution (RTE) in Zeeman-induced polarization regime. Like other inversion codes gives us the physical parameters (temperature, magnetic field vector, gas and pressure density and other ones) of the atmosphere where the Stokes profiles were formed.

3. Results

Fig. 1 displays three examples of the observed and inverted Stokes profiles, relevant to the penumbra. These plots show a good match of the inverted profiles with the observed ones,
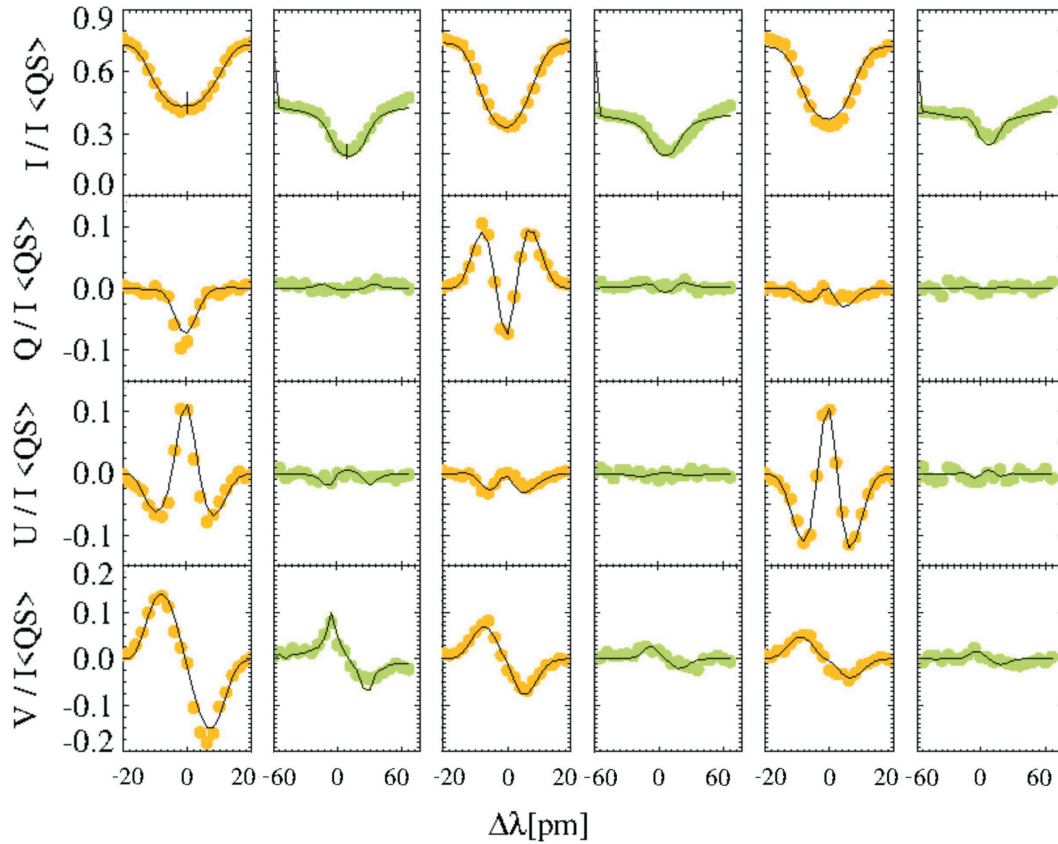
Figure 1. Examples of observed (filled yellow/green circles) and inverted (black solid line) Stokes profiles in the studied penumbra. The yellow and green profiles represent the Fe I 617.3 nm and Ca I 854.2 nm line profiles, respectively. In each column the 0 in the x-axis indicates the line core position of the two lines, 617.32 nm and 854.04 nm, respectively.

especially for the Fe I data which have strong Q, U and V signals. Although the Q and U signals measured in Ca II are lower, they are above the noise level of the data. Fig. 2 shows the maps of the magnetic field strength (first and third rows) and inclination of the magnetic field (second and fourth rows) for different atmospheric layers (reported as function of the optical depth τ) as derived from our multi-line inversion in two regions in the southern and northern part of the penumbra, respectively. [1] reported the study of the response function of both observed lines in order to consider the retrieved physical parameters at the maximum of sensitivity range. In this respect, the maps shown in Fig. 2 refer to three photospheric layers and one chromospheric height as derived from the analysis of the Fe I 617.3 nm and Ca II 854.2 nm lines, respectively. The three photospheric heights ($\log \tau^1$ =-0.5, -1 and -1.5) exhibit the well known spine-intraspine structure in the maps of both the magnetic field strength and magnetic field inclination.

The maps at $\log \tau$ =-1 display the small-scale variation better than the maps at the other two photospheric heights. In particular, at $\log \tau$=-0.5 and -1 the maps of the magnetic field

---

[1] where $\log \tau$=-0.5,-1 and -1.5 represent the lower, medium and upper solar photosphere.

inclination exhibit an interlaced radially regular distribution of alternate, more vertical and more horizontal fields. This structure is still visible in the chromospheric maps ($log\tau$=-4.6), even though with different values (≈ 1.2 kG and $\approx 70°$ compared to ≈ 1.6 kG and $\approx 60°$ at $\log\tau$=-1). We analyzed the azimuthal variation of the magnetic field quantities by considering three arcs, from the inner to the outer part of the penumbra (see the arcs A1, A2 and A3 drawn in the continuum image of Fig. 3, left panel). In particular, A1 lies in the outer penumbra while A2 and A3 in the inner part of the penumbra. Moreover, A1 and A2 sample penumbral regions where the filaments are uniformly arranged, while the A3 arc comprises inhomogeneous filaments in the southern part of the penumbra. The studied quantities in the outer penumbral filaments (see the plot of Fig. 3 relevant to the A1 arc) exhibit slight variations, but still detectable, of the small-scale spine-intraspine structure. At the two photospheric heights $\log\tau$=-1 and -1.5 we found interlaced variations of the LOS magnetic field of ≈ 300 G, which decreases to $\approx 150 - 200$ G at chromospheric height. The LOS field variations along A2 and A3 are similar to the behaviour seen along A1, but with higher field strength values. The bottom right panels of Fig. 3 display the variation of the magnetic field inclination along the three arcs. In the inner penumbra this parameter changes while passing from the photosphere to the chromosphere, with a decrease of the peak-to-peak variation of $\approx 10°$ (see the variation along the A3 arc). It is worthwhile noting that the magnetic field appears more vertical in the chromosphere: this can be explained as an evidence that we observed the magnetic canopy[2] at different heights. The variation of the inclination angle observed in the chromosphere resembles that retrieved in the photosphere. The peak-to-peak variation along the A1 arc from the photosphere to the chromosphere is $\approx 55° - 60°$ and up to $90°$, respectively.

Following [17], we derived the vertical gradient of the magnetic field. The photospheric gradient (calculated between $\log\tau$=-0.5 and $\log\tau$=-1.5) displays a ring-like structure in the inner penumbra, where the gradient has negative values, i.e., the field decreases with optical depth. The outer penumbra shows positive values of the photospheric gradient instead. We also estimated the field gradient between the photosphere and the chromosphere (considering as photosphere the height where the sensitivity of our measurements is higher, i.e., $\log\tau$=-1). The results confirm the previous value reported by [10].

4. Conclusions

The results discussed above derive from the analysis of data acquired at spectral ranges never explored before for the study of the penumbra structure. Analyzing spectro-polarimetric measurements of the solar atmosphere along Fe I 617.3 nm and Ca II 854.2 nm lines, we studied the magnetic field strength and inclination of a sunspot penumbra. Our findings clearly show the well known spine-intraspine structure at all the atmospheric heights considered, although in the chromosphere the structure is less evident.

Recently, the penumbral magnetic field structure in the upper chromosphere has been derived from GREGOR observations in the spectral region of the He I triplet [18]. Their observations revealed an azimuthal variation of the magnetic field inclination resembling the photospheric spine-intraspine structure. In our case, both the magnetic field strength and inclination angle exhibit small scale variations. According to [19], the joint analysis of the Fe I and Ca II lines can greatly enhance the sensitivity of the analyzed data to the atmospheric parameters at lower heights.

The photospheric field gradient exhibits a ring-like structure in the inner penumbra as reported by [10]. Furthermore, from the comparison between the photospheric and chromospheric magnetic field, we found for the vertical gradient a value of 100 G/$\log\tau$,

---

[2] The field in the magnetic elements (pores or sunspots) is bent over as these expand. This particular field configuration where nearly horizontal field lines are located over a region with weaker (or no) field is called magnetic canopy [15]
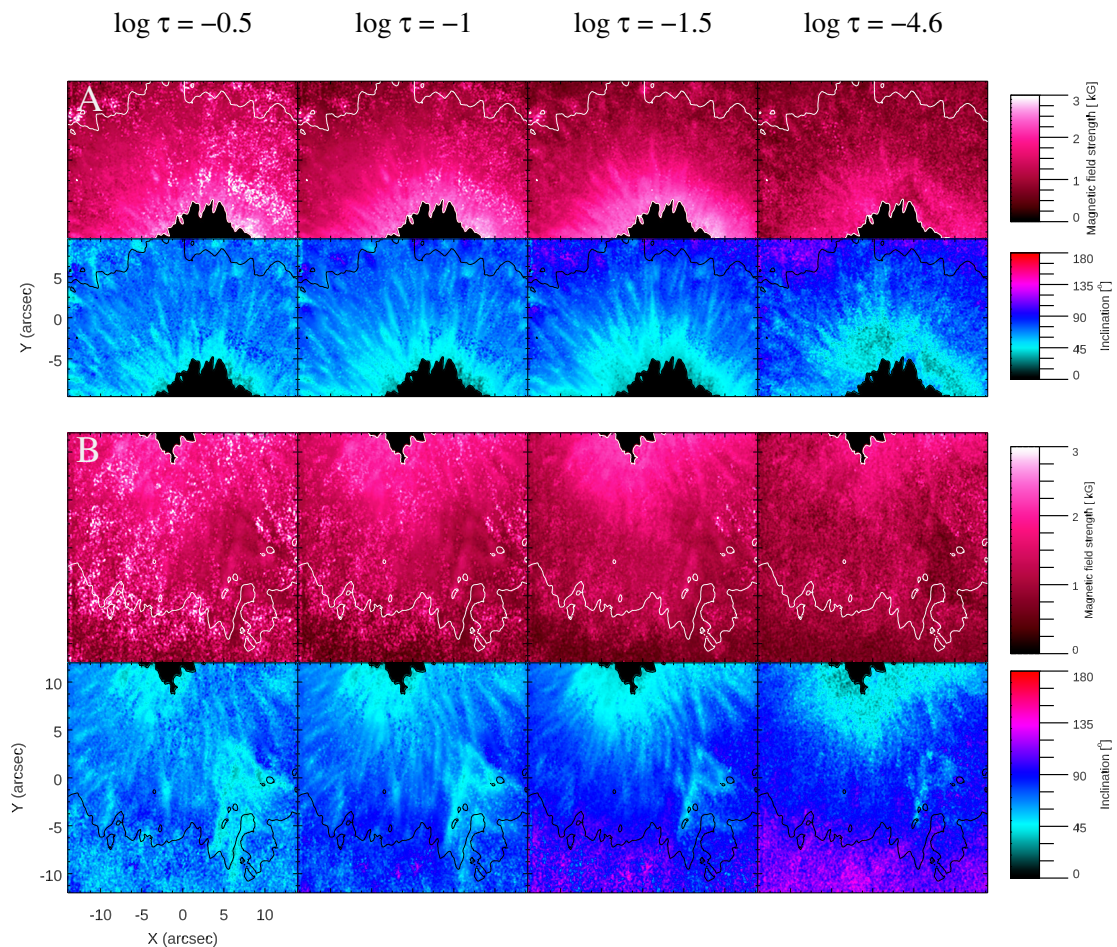
Figure 2. Maps of the magnetic field strength (top panels) and inclination of the magnetic field (bottom panels) over two penumbral sectors. From left to right, the maps show the quantities at three different photospheric layers and in the chromosphere. The 0° and 180° values define the direction of the magnetic field toward or away the observer, rispectively.

corresponding to a variation of ≈ 0.3 Gkm^{-1}. This value is in agreement with previous similar estimates [10, 20].

In order to obtain a complete reconstruction of the magnetic field in the penumbral filaments at higher atmospheric heights other data are needed, as well as simultaneous observations by using multiple spectral diagnostics of the photosphere and chromosphere. The already operative CRISP/CHROMIS spectro-polarimeters working in the near ultraviolet and visible bands can provide those data, as well as the future instrumentation that will be offered by the next generation 4-m class solar telescopes, such as the Daniel K. Inouye Solar Telescope [21] and European Solar Telescope [22] close to first-light and under design phase, respectively.
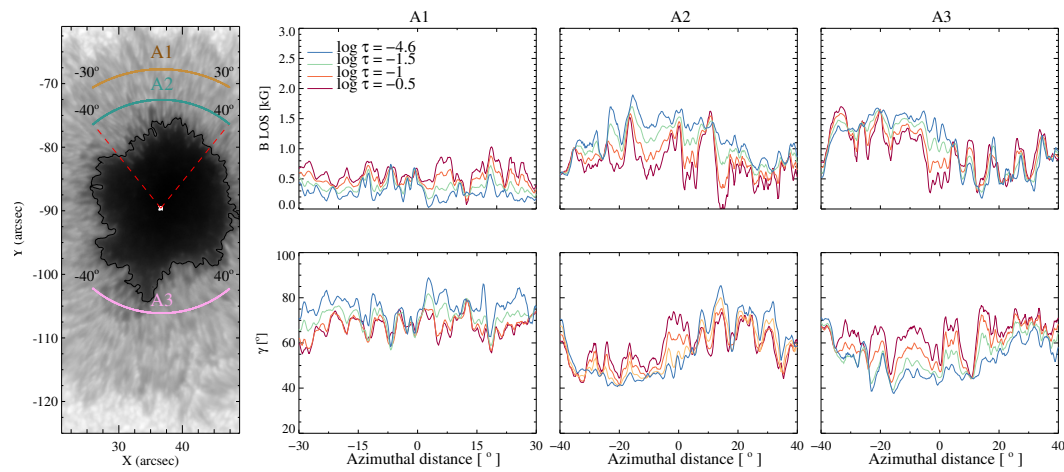
Figure 3. Left panel: continuum map of AR NOAA 12546. Right panels: Variation of the LOS magnetic field (top panels) and inclination of the magnetic field (bottom panels) along the three arcs A1, A2 and A3 drawn in the continuum map. The different colors, displayed in the legend, represent the values obtained at four different $\log \tau$.

References
[1] Murabito M, Ermolli I, Giorgi F, *et al.* 2019 *Astrophys. J.*, **873**, 126
[2] Romano P, Frasca D, Guglielmino S L, *et al.* 2013 *Astrophys. J.* **771** L3
[3] Romano P, Guglielmino S L, Cristaldi A *et al.* 2014 *Astrophys. J.* **784** A10
[4] Murabito M, Romano P, Guglielmino S L, Zuccarello F and Solanki S K 2016 *Astrophys. J.* **825** 75
[5] Murabito M, Zuccarello F, Guglielmino S L, and Romano P 2018 *Astrophys. J.* **855** 58
[6] Schlichenmaier R, Rezaei R, Bello González N, and Waldmann T A 2010 *Astron. Astrophys.* **512** L1
[7] Murabito M, Romano P, Guglielmino S L, and Zuccarello F 2017 *Astrophys. J.* **834** 76
[8] Tiwari S K, van Noort M, Lagg A, and Solanki S K 2013 *Astron. Astrophys.* **557** A25
[9] Joshi J, and de la Cruz Rodríguez J 2018 *Astron. Astrophys.* **619** A63
[10] Joshi J, Lagg A, Hirzberger J, and Solanki S K 2017 *Astron. Astrophys.* **604** A98
[11] Cavallini F 2006 *Sol. Phys.* **236** 415
[12] Stangalini M *et al.* 2018 *Astrophys. J.* **869** 110
[13] Socas-Navarro H, de la Cruz Rodríguez J, Asensio Ramos A, Trujillo Bueno J, and Ruiz Cobo B 2015 *Astron. Astrophys.* **577** A7
[14] Robustini C, Leenaarts J, and de la Cruz Rodríguez J 2018 *Astron. Astrophys.* **609** A14
[15] Jafarzadeh S, Rutten R J, Solanki S K, *et al.* 2017 *Astrophys. J. Suppl. S.* **229** 11
[16] Fontenla J M, Avrett E H, and Loeser R 1993 *Astrophys. J.* **406** 319
[17] Joshi J, Lagg A, Hirzberger J, and Solanki S K, and Tiwari, S K 2017 *Astron. Astrophys.* **599** A35
[18] Joshi J, Lagg A, Solanki S K, *et al.* 2016 *Astron. Astrophys.* **596** A8
[19] Quintero Noda C, Shimizu T, Katsukawa Y, *et al.* 2017 *Mon. Not. R. Astron. Soc.* **464** 4534
[20] Balthasar H, 2018 *Sol. Phys.* **293** 120
[21] Keil S L, Rimmele T R, Wagner J, and ATST Team 2010 *Astron. Nachr.* **331** 609
[22] Collados M, Bettonvil F, Cavaller L, and EST Team 2010 *Astron. Nachr.* **331** 615